Science Advances
AAAS

Supplementary Materials for

Entangling free electrons and optical excitations

Andrea Konečná *et al.*

Corresponding author: F. Javier García de Abajo, javier.garciadeabajo@nanophotonics.es

Sci. Adv. **8**, eabo7853 (2022)
DOI: 10.1126/sciadv.abo7853

This PDF file includes:

Figs. S1 to S6

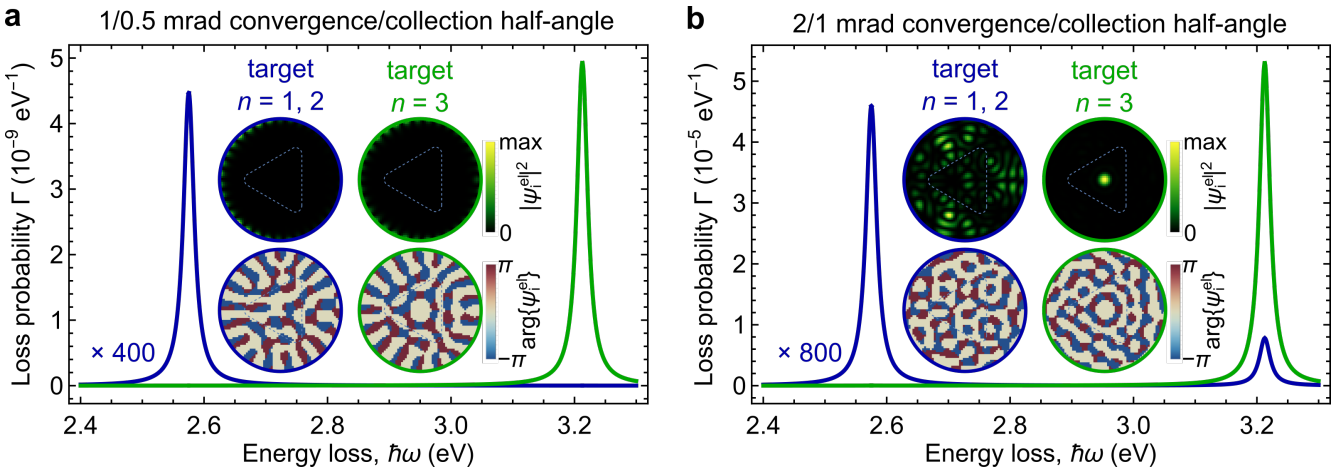

FIG. S1. **Selective excitation of plasmon modes in a silver nanotriangle.** Same as Fig. 2(c) in the main text (a) for incidence and collection half-angles $\varphi_i = 1$ mrad and $\varphi_f = 0.5$ mrad respectively; and (b) for $\varphi_i = 2$ mrad and $\varphi_f = 1$ mrad.

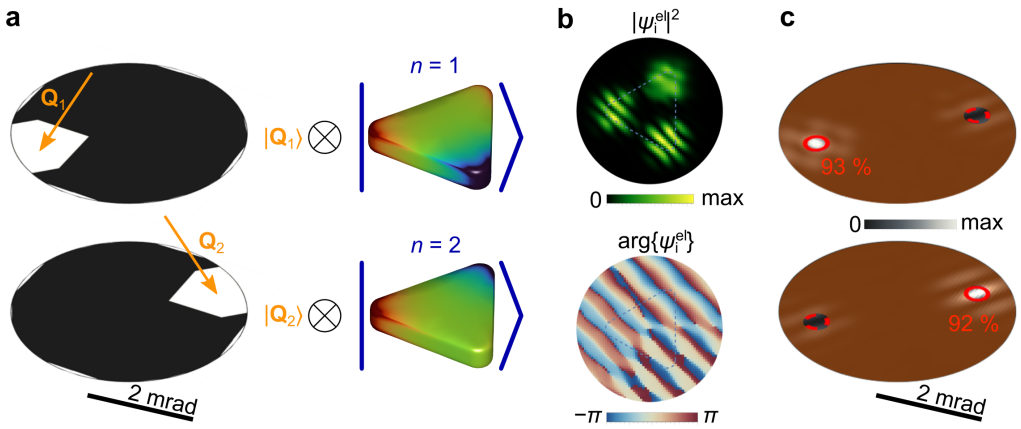

FIG. S2. **Creation of electron-sample entanglement by direct inversion.** This figure shows a similar analysis as Fig. 3 in the main text, but panel (a) indicates that the total number of pixels is reduced to 13 to ease the calculation, so that the apertures are represented by 1 pixel each. Also, panels (b) and (c) are now obtained by direct inversion of Eq. (7) with $\alpha^f_{\mathbf{Q}_f,n}$ set to 1 in the target aperture and 0 otherwise. In (c), each aperture (small circles) transmits the indicated fraction of the targeted excitation n.

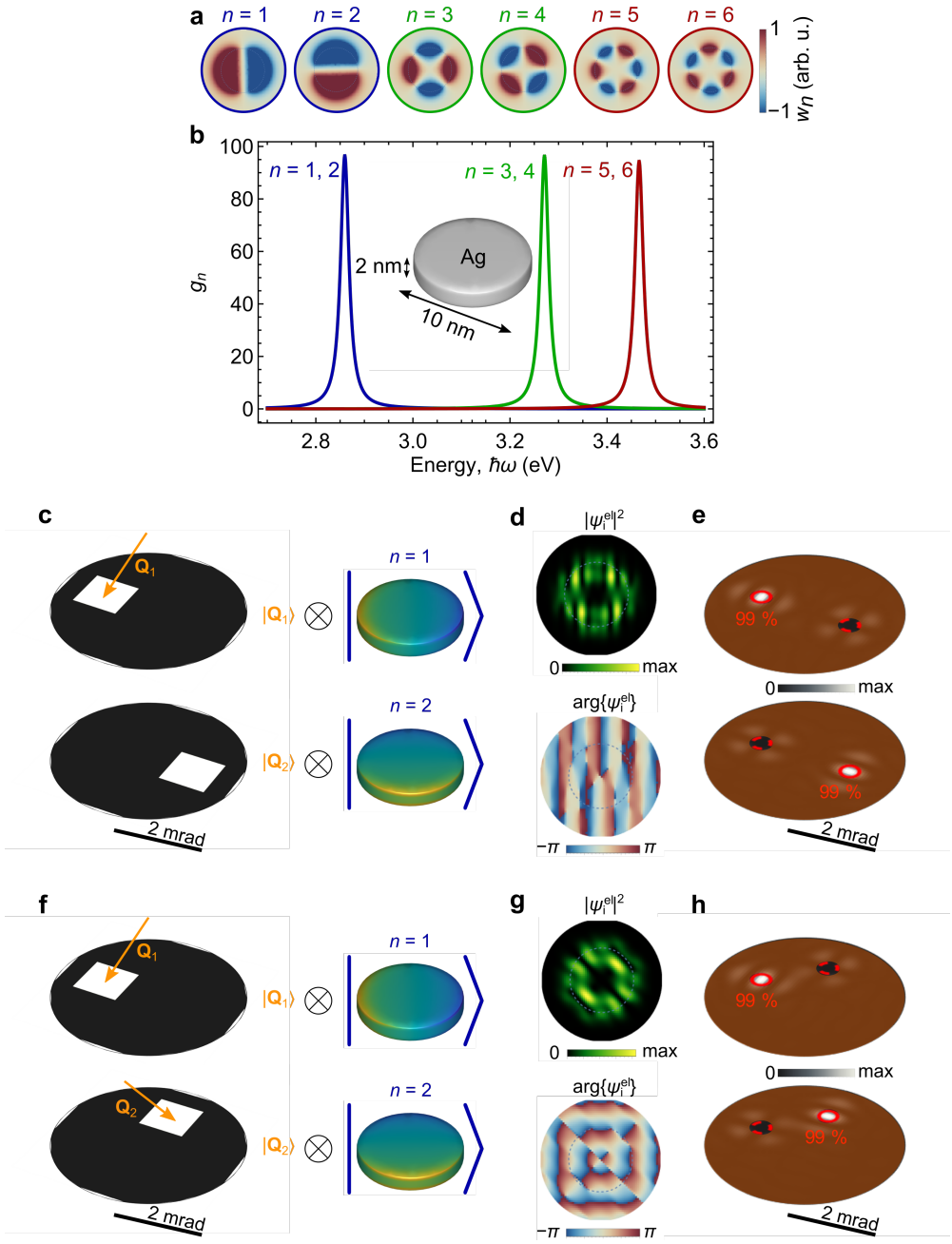

FIG. S3. **Creation of electron-sample states with a high-degree of entanglement using a silver nanodisk.** (a,b) Spatial profiles (a) and spectral functions (b) associated with plasmons in a silver disk (2 nm thickness, 10 nm diameter). Degenerate modes are denoted by the same color in the frame, curve, and label. (c) Pursued electron-sample entangled states, consisting of the superposition of selected (by means of two apertures) electron-momentum states within the white pixels in $\mathbf{Q}_f$ space (left) and correlated degenerate dipolar plasmons in the silver nanodisk (right). (d) Spatial profile of the optimized incident wave function $\psi_i^{\mathrm{el}}(\mathbf{R})$ required to produce the final state in (c). The disk contour is indicated with dashed circumferences. (e) Resulting probability distributions $\left|\langle \mathbf{Q}_f, n|\Psi_f\rangle\right|^2$ with $n = 1$ (top) and $n = 2$ (bottom) in $\mathbf{Q}_f$ space, where each aperture (small circles) transmits the indicated fraction of the targeted excitation n. (f,g,h) Same as (c,d,e), but for a different location of $\mathbf{Q}_2$. The area outside the apertures in (e) and (h) (intended to be masked) is colored to emphasize the selected momentum regions of interest. The optimization is carried out for 100 keV electrons, 81 detector pixels in each of the two apertutes (around $\mathbf{Q}_1$ and $\mathbf{Q}_2$), $\varphi_i = 4\,\mathrm{mrad}$, and $\varphi_f = 2\,\mathrm{mrad}$.

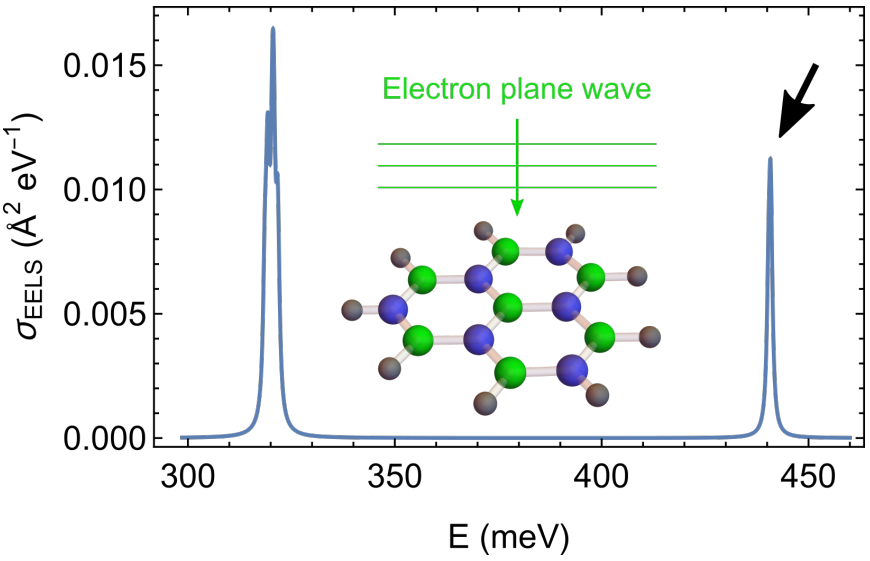

FIG. S4. **Spectrally resolved EELS cross section for the hBN-like molecule considered in Fig. 4 of the main text.** We take the electron to be incident normal to the atomic plane of the molecule.

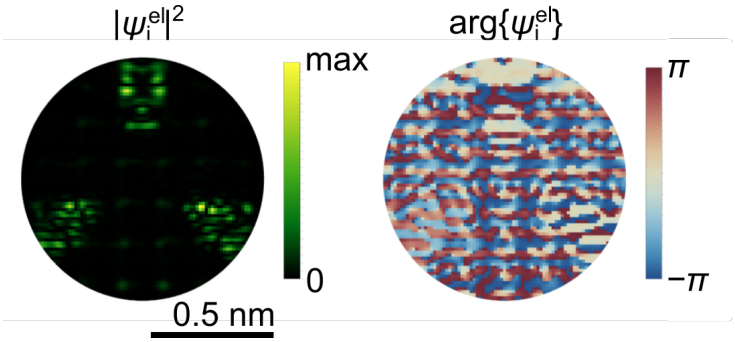

FIG. S5. **Entanglement of free electrons and atomic vibrations.** Optimized incident electron wave function $\psi_i^{\mathrm{el}}(\mathbf{R})$ required to produce the entangled state shown in Fig. 4 of the main text.

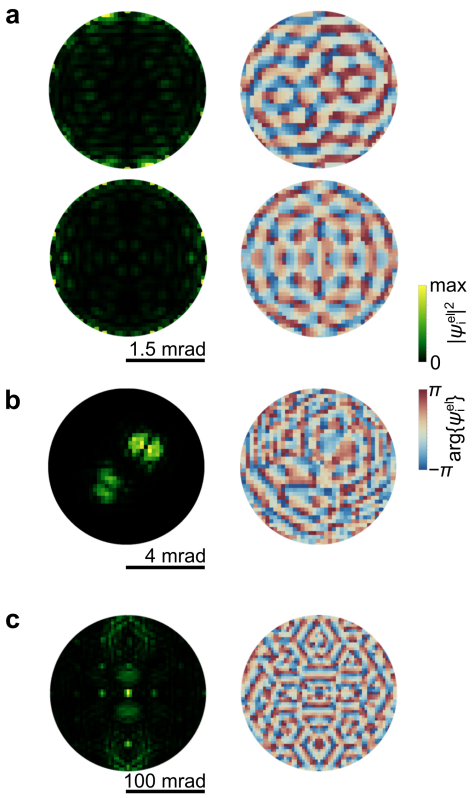

FIG. S6. **Entanglement of free electrons and plasmons in nanoparticles.** Optimized incident wave functions $\psi_i^{\mathrm{el}}(\mathbf{Q}_i)$ in $\mathbf{Q}_i$ space corresponding to different calculations in this work: panels (a,b) relate to Figs. 2(c) and 3(b) in the main text, respectively, and panel (c) to Supplementary Fig. S5.